COMPDYN 2013
4th ECCOMAS Thematic Conference on
Computational Methods in Structural Dynamics and Earthquake Engineering
M. Papadrakakis, V. Papadopoulos, V. Plevris (eds.)
Kos Island, Greece, 12–14 June 2013

INFLUENCE OF STRUCTURAL PERIODICITY ON VIBRATION TRANSMISSION IN A MULTI-STOREY WOODEN BUILDING

Lars V. Andersen

Aalborg University, Department of Civil Engineering
Aalborg, Denmark
e-mail: la@civil.aau.dk

Keywords: Finite element analysis, steady-state response, transient response, periodic structure, substructure.

Abstract. *Noise is a nuisance to people, and buildings should therefore be designed to prevent propagation of sound and vibration in the audible frequency range as well as the range of frequencies relevant to whole-body vibrations of humans. In heavy structures made of concrete and masonry, a source with high energy content is required to mobilise the inertia. However, for lightweight building structures made of wood, less energy is required to produce vibrations since the mass is smaller. This leads to a high risk of sound and vibration propagation in terms of direct as well as flanking transmission.*

However, lightweight structures are typically periodic in the sense that joists and studs are placed with a repetition of the same distance along each panel. Further, in a multi-storey building the geometry of entire rooms may be repeated along the horizontal and vertical directions. Such periodicity is known to result in pass bands and stop bands regarding wave propagation. The paper focuses on analysing and quantifying the effects that a change in the structure, especially regarding the periodicity, has on the overall dynamic performance in the low to mid frequency range up to 250 Hz.

The analysis is performed by means of a finite-element model. Firstly, a rigorous solid finite-element model is made for each wall and floor panel. Secondly, reduced models with significantly fewer degrees of freedom are obtained by component mode synthesis, augmenting Guyan reduction with a number of internal Eigen modes. Using a substructure approach, the panels are then combined to a global model of a multi-storey building. Example Eigen modes of a single floor panel and the global building are presented. Vibration caused by point force excitation is finally analysed in the frequency domain as well as the time domain.

1 INTRODUCTION

Noise and vibration are critical factors regarding human comfort in the built environment. With increasing population density in cities follows a demand of designing buildings with focus not only on structural strength and safety, but also on indoor comfort and sustainability. In this context, timber has number of advantages, but also some shortcomings. With recent advances in structural engineering it has become possible to construct large multi-storey wooden buildings. However, a reliable assessment of sound and vibration transmission in such buildings in the early design phase cannot be carried out by the methods developed for heavy structures made of concrete or masonry. Thus, statistical energy analysis (SEA) [1] and the European standard EN12354-1 [2] have been found to provide inaccurate results for lightweight structures [3]—especially in the low and mid-frequency range.

Regarding the analysis of lightweight wooden building structures, one of the main shortcomings of SEA and related methods lies in the fact that a uniform modal density is assumed. This is contradictory to the dynamic properties of wooden structures. The inherent periodicity of mass and stiffness due to studs and joists in wall and floor panels leads to the existence of pass bands and stop bands for transmission of elastic waves [4]. Whereas this may complicate dynamic analysis, it may, on the other hand, be utilized in the design of a building to avoid transmission of vibration and sound within certain frequency ranges from, for example, foot steps, unbalanced washing machines, air conditioning or elevator motors.

To quantify the effects of periodicity, a finite-element (FE) model is applied in the present paper. FE models have been used for analysis of wooden structures by, among others, Brunskog and Davidsson [5], Løvholt et al. [6], Maluski and Gibbs [7], and Fiala et al. [8]. For large building structures, a solid FE model will contain millions of degrees of freedom if individual joist and studs are to be modelled in detail. Hence, parametric studies become very time consuming. However, Andersen et al. [9] proposed the use of a modular FE model in which the walls and floors are treated as substructures, leading to a significant reduction of the number of degrees of freedom. This approach is employed in the present paper for dynamic analysis of two-storey buildings with different numbers of modules in the length direction and with different distances between the joists and studs. The Eigen modes of the various structures are identified, and analyses of the steady state response to harmonic loading is carried out in the frequency domain within the range 0–250 Hz. Finally, a time-domain analysis is performed to quantify the transient displacement response to a step load on one of the floors.

2 THE COMPUTATIONAL MODEL

2.1 Modular finite-element building model

A finite-element (FE) model of a lightweight wooden building structure has been made, based on a modular approach using substructures for each wall and floor panel. Figure 1 illustrates the overall geometry and principle of the model. The example building shall be named "House 4-3-2" since it is 4 modules long in the x-direction, 3 modules high in the y-direction and 2 modules wide in the z-direction. The module lengths in the x, y and z-directions are denoted L, H and W, respectively. Further, as shown in the figure, rooms and panels are number in accordance with their position within the model. For example, y-Wall 1-2-1 is the first wall in the x and z-directions, and the second wall in the y-direction, with an orientation along the z-axis, cf. Figure 1.

The FE model has been developed with the commercial software code Abaqus 6.12-2 [10] using Python scripting to allow parametric studies in an efficient manner. Firstly, each of the

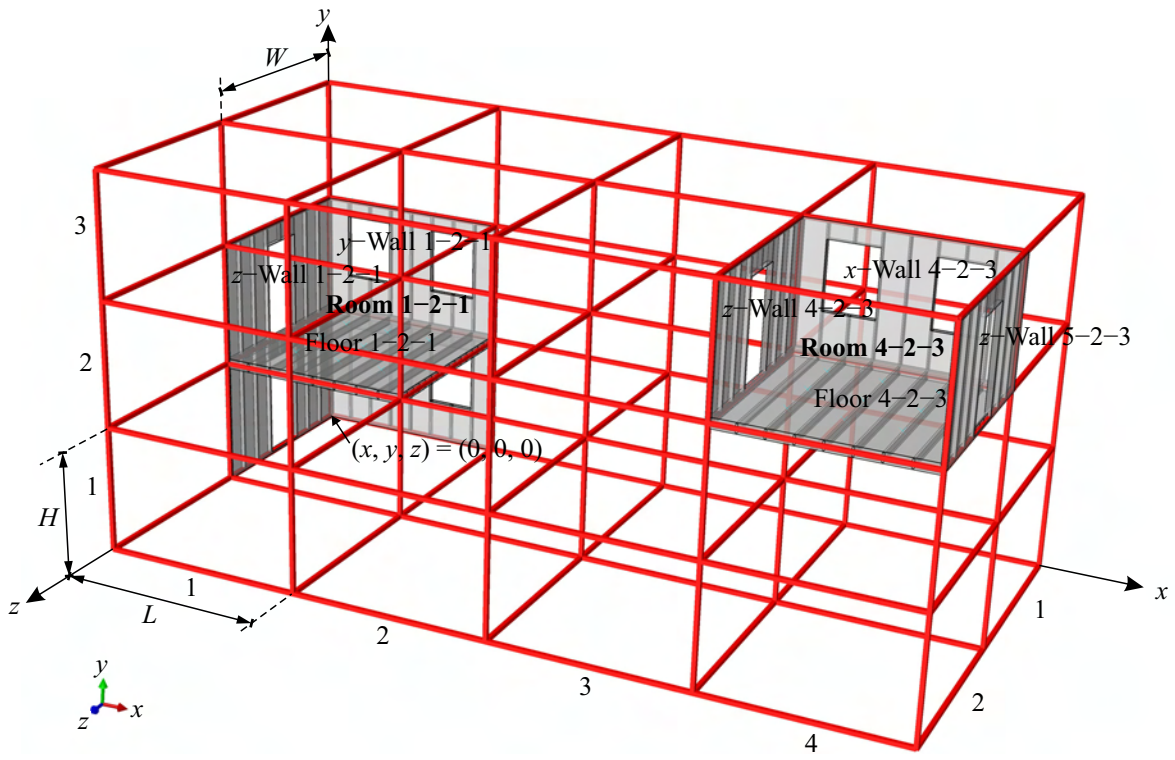

Figure 1: Definition of modular finite-element building model for House 4-3-2.

wall and panels has been modelled in high detail using 20-node solid brick finite elements with full integration and quadratic interpolation of the displacement field. A regular structured hexahedral mesh with a mesh size of maximum 100 mm has been utilized to obtain results of high accuracy in the frequency range below 500 Hz.

The walls are made as double-leaf single-stud panels, assuming all connections to be glued, i.e. fully tied. The plate thickness is 15 mm, whereas the studs are 100 mm thick and 45 mm wide, leading to a total wall thickness of 130 mm. In all considered models within the present analyses, the height of each wall panel is 3.00 m, and the z-wall panels parallel to the (y, z)-plane all have a width of $W = 4.80$ m. The same width applies to the floor panels in all models. Like the walls, the floors are double-leaf single-joist panels. However, the plates are 20 mm thick and the joists have a cross-sectional area of 200×45 mm^2, resulting in a total floor thickness of 240 mm. A 45 mm wide solid frame is placed along the edges of all panels, again assuming glued connections.

As indicated in Figure 1, 1200×1600 mm^2 (length $\times$ height) window openings are cut into the x-wall panels that form the facade of the building along the x-direction. The first window in every panel is placed 600 mm from the end of the panel along the x-direction and 1000 mm from its base along the y-direction. Depending on the length of the wall module, a number of repetitions are made with a distance of 1200 mm between windows in the x-direction. Likewise, a single door opening is made in the middle of the z-walls with a height of 2445 mm and a width of 1200 mm. The opening is placed 45 mm (the width of the frame) above the base of the wall.

Construction wood and plywood are idealized as an isotropic, linear viscoelastic material with Young's modulus $E = 9.5$ GPa, Poisson's ratio $\nu = 0.3$, mass density $\rho = 455$ kg/m^3. Material dissipation is defined in terms of Rayleigh coefficients providing damping ratios of 2% at 10 Hz and 100 Hz. As a result, a minimum damping ratio of 1.14% occurs at 31.6 Hz.

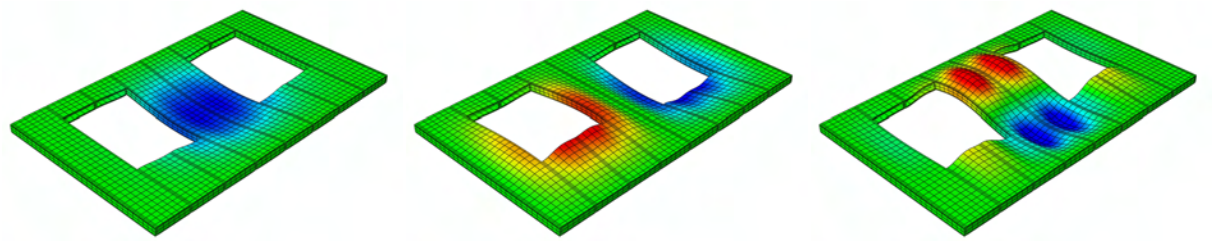

Mode 1 @ 72 Hz Mode 2 @ 98 Hz Mode 7 @ 164 Hz

Figure 2: Example Eigen modes and Eigen frequencies of x-wall panel module with two window openings. The panel dimensions are $(L \times H) = (4.80 \times 3.00)$ m^2, and the joist distance is 600 mm. Red and blue shades indicate positive and negative out-of-plane displacements, respectively.

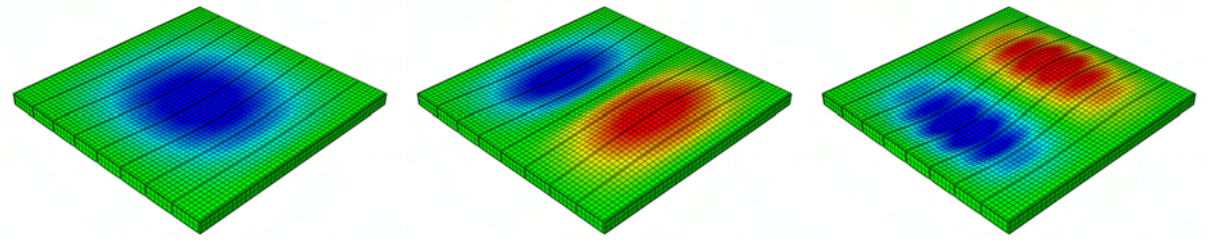

Mode 1 @ 58 Hz Mode 2 @ 69 Hz Mode 7 @ 138 Hz

Figure 3: Example Eigen modes and Eigen frequencies of y-floor panel module. The panel dimensions are $(L \times W) = (4.80 \times 4.80)$ m^2, and the joist distance is 600 mm. Red and blue shades indicate positive and negative out-of-plane displacements, respectively.

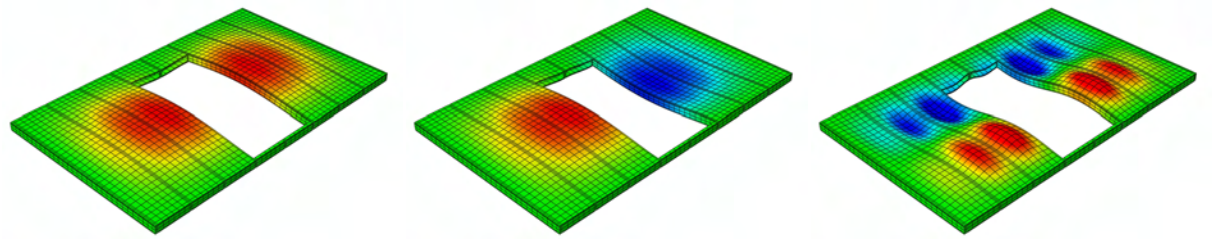

Mode 1 @ 73 Hz Mode 2 @ 73 Hz Mode 7 @ 163 Hz

Figure 4: Example Eigen modes and Eigen frequencies of z-wall panel module with door opening. The panel dimensions are $(W \times H) = (4.80 \times 3.00)$ m^2, and the joist distance is 600 mm. Red and blue shades indicate positive and negative out-of-plane displacements, respectively.

Material dissipation of this magnitude is judged to be realistic for wood. However, for a building including joints and nonstructural elements, e.g. insulation material, it may be unrealistically low. Therefore, in the response predicted by the present FE model may be less damped than the response of a real structure.

Example mode shapes and corresponding Eigen frequencies for an x-wall panel with dimensions $(L \times H \times W) = (4.80 \times 3.00 \times 4.80)$ m^3 and stud distance 600 mm are illustrated in Figure 2. In accordance with the explanation above, two windows are present in this panel. Likewise, Figure 3 shows three modes and the related Eigen frequencies for a floor panel with dimensions $(L \times W) = (4.80 \times 4.80)$ m^2 and joist distance 600 mm, whereas Figure 4 provides an illustration of three modes in a z-wall panel with dimensions $(W \times H) = (4.80 \times 3.00)$ m^2 and stud distance 600 mm. It can be seen in Figures 2 and 4 that the first Eigen mode of each wall occurs at a frequency of about 72–73 Hz, whereas the fundamental mode of the floor occurs at 58 Hz, in all cases assuming that the panels are fully fixed along the edges. These frequencies may be slightly high, but it should be noted that nonstructural mass has been disregarded.

Before assembly of the global building FE model, a system reduction is carried out in order to provide a substructure, i.e. a macro finite element, for each of the wall and floor panels. In the present analyses, nodes are retained along the edges of the panels for every 300 mm. For example, 17 nodes are retained along each side of a floor panel with dimensions $(L \times W) = (4.80 \times 4.80)$ m^2, including two corner nodes. It is noted that only the nodes in the midplane of the panel are retained. However, to allow a coupling of the rotational degrees of freedom from one panel to another, rigid shell elements are introduced in the cross sections of the panel frame at the position of the retained nodes. Hence, six degrees of freedom are retained at each node.

Especially, in the floor panels, additional nodes are retained on the top surface of the floor. These nodes are placed in a grid with the mesh size 1200×1200 mm^2, providing, e.g., an additional $3 \times 3 = 9$ nodes on a 4.80×4.80 m^2 floor panel. The purpose of the nodes placed on the top surface of the floors is to allow application of concentrated forces or discrete nonstructural masses at these positions. Since no external moments or mass moments of inertia are to be applied, only the translational degrees of freedom are retained at the additional nodes.

Taking the approach of Craig and Bambton [11] (see also Ref. [12]), the system matrices achieved by Guyan reduction [13] of the system matrices are enriched by a number of internal modes of a model fixed at the retained degrees of freedom. All modes up to a frequency of 400 Hz are included in the substructures in order to provide an acceptable accuracy of the global model up to 250 Hz. The result of the system reduction is a substructure for each panel with 300 to 600 degrees of freedom. This should be compared to the original 90,000 to 250,000 degrees of freedom present in the rigorous models of the panels. Nonetheless, a very high computational accuracy is maintained.

The individual panels are combined to form a building with a number of rooms in each of the x, y and z-directions. In the present version of the modular FE model, all x-walls are identical, e.g. x-Wall 3-2-1 is identical to x-Wall 2-1-2. The same limitation applies to floor and z-wall panels. Following the idea of Kiel et al. [14], all panels are attached to an artificial skeleton made of beam finite elements as sketched in Figure 1. The skeleton nodes act as a common master, and the retained nodes of the panels act as slaves within the Abaqus "tie" definition. To ensure that the skeleton will not influence the overall behaviour of the building model, the skeleton has a very low stiffness. Further, to avoid spurious modes of resonance in the skeleton within the considered frequency range up to 250 Hz, the beams have a very low mass. In the present case, 3-node Mindlin beam elements with a node distance of 300 mm, a cross-sectional area of 10×10 mm^2, a mass density of 1 kg/m^3, and a Young's modulus of 1 GPa are applied.

Nonstructural mass is included to obtain resonance frequencies of the FE model that more realistically represent the behaviour of a real building. Thus, a discrete mass of 100 kg is applied at each of the retained nodal points on the top surface of the floor panels. As an example of a final model, Figure 5 shows House 3-2-1 with module lengths $(L \times H \times W) = (4.80 \times 3.00 \times 4.80)$ m^3 and a rib distance of 600 mm. This model has a total of 24,940 degrees of freedom. Example Eigen modes are shown in Figure 6.

By inspection of Figure 6 it can be seen that the first modes of resonance related to vibrations in the z-direction (Mode 1), the x-direction (Mode 2), and torsion about the y-axis (Mode 9) lie very close for the present building. This is expected since the x-walls and z-walls have similar stiffnesses regarding bending as well as in-plane shear. Further, it is observed that the first local modes of bending in the floor panels occur between the first three global modes of resonance. Actually, a total of six such local floor modes exist at a frequency of 19 Hz, but only one of the modes is visualized in the figure.

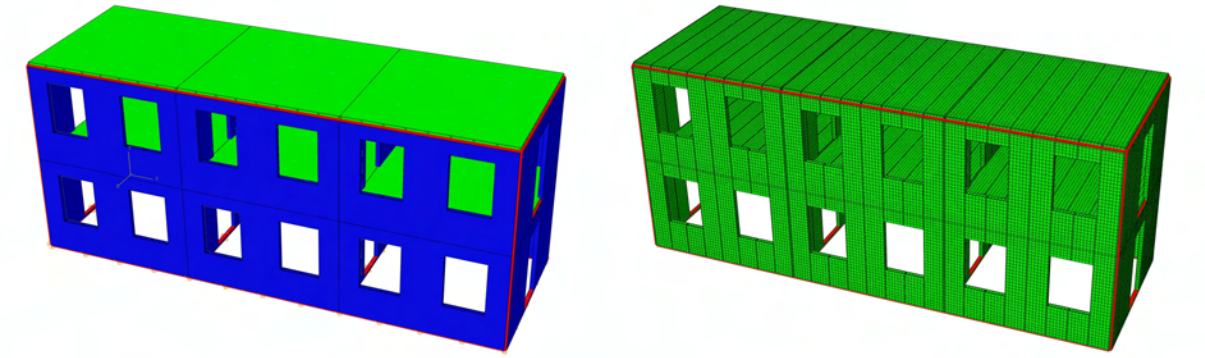

Figure 5: Example of a modular finite-element building model. Left: House 3-2-1 with module lengths $(L \times H \times W) = (4.80 \times 3.00 \times 4.80)$ m^3 and rib distance 600 mm. Wall panels are blue, floor panels are green, and the artificial skeleton is red. Right: Finite-element mesh (mesh size $\leq$ 100 mm).

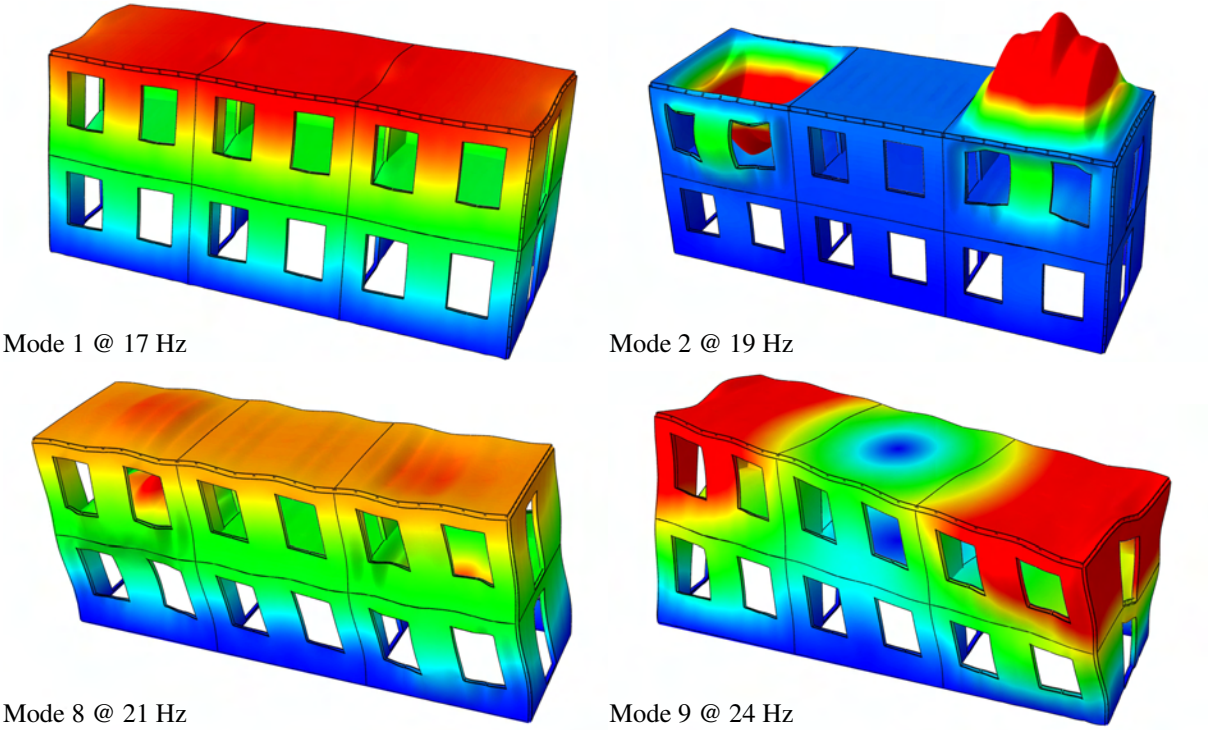

Mode 1 @ 17 Hz

Mode 2 @ 19 Hz

Mode 8 @ 21 Hz

Mode 9 @ 24 Hz

Figure 6: Example Eigen modes and corresponding Eigen frequencies of House 3-2-1 with the module size $(L \times H \times W) = (4.80 \times 3.00 \times 4.80)$ m^3 and rib distance 600 mm. Red, green and blue shades indicate large, moderate and no displacements, respectively.

2.2 Analyses

Three different comparisons are made in order to analyse the influence of changes in the inherent periodicity due to ribs in the panels or repetitions of rooms along the building:

1. The response of three variants of House 2-2-1 is analysed. The module size is $(L \times H \times W) = (4.80 \times 3.00 \times 4.80)$ m^3 in all three models, but different rib distances of 600, 400 and 300 mm are applied.

2. The response of five buildings with two storeys and one room in the width direction is assessed. The numbers of rooms in the length direction are 2, 3, 4, 5 and 6, respectively. The module size is $(L \times H \times W) = (4.80 \times 3.00 \times 4.80)$ m^3, and the distances between studs and joists are 600 mm.

3. Three buildings with two storeys, one room in the width direction and a total length of 14.40 m are considered. The module height is $H = 3.00$ m and the module width is $W = 4.80$ m in all three models. The module lengths are $L = 7.2$ m, $L = 4.8$ m and $L = 2.4$ m, respectively, leading to 2, 3 or 6 rooms along the building.

In each comparison, three analyses are carried out. Firstly, the undamped Eigen frequencies and the related Eigen modes are identified in the frequency range 0–250 Hz with the purpose of quantifying the modal density related to each building. The Lanczos solver available in Abaqus has been utilized. Secondly, direct steady state analysis is performed in the frequency domain in order to investigate the response of the buildings to vertical harmonic excitation at a point on one of the floors. Again the frequency range 0–250 Hz is considered. Thirdly, the transient response to a step load in the same position as the harmonic force is studied. The load is defined with a smooth amplitude function having the values 0 N at 0 ms, 1 N at 5 ms and 0 N 10 ms. The smoothing implies that the first and second time derivatives of the amplitude function are zero at the instants 0, 5 and 10 ms where the load values are specified [10]. Time integration is performed by the Newmark scheme [15] with a time increment of 0.5 ms.

Results of the transient response obtained in the time domain will be presented in terms of vertical displacements at selected points within the respective buildings. The results in the steady state analyses are evaluated in terms of root-mean-square (RMS) velocities of the retained nodes on the floor in a given room:

$$\langle V \rangle_{\mathrm{RMS}} = \sqrt{\frac{1}{N} \sum_{n=1}^{N} \mathbf{V}_n^H \mathbf{V}_n}, \tag{1}$$

where N is the number of restrained nodes on the floor top surface, whereas $\mathbf{V}_n$ is the complex velocity amplitude vector at node n, and $\mathbf{V}_n^H$ denotes its conjugate transpose. The RMS velocities are evaluated in decibel according to the definition:

$$\langle V \rangle_{\mathrm{RMS}}^{\mathrm{dB}} = 20 \log_{10} \left(\frac{\langle V \rangle_{\mathrm{RMS}}}{V_0} \right), \quad V_0 = 1 \text{ nm/s}. \tag{2}$$

The loss in dB from one room to another can be found, simply, by subtracting the value of $\langle V \rangle_{\mathrm{RMS}}^{\mathrm{dB}}$ in the receiver room from the corresponding value in the source room.

3 Results and discussion

3.1 Eigen frequencies of finite-element building models

Figures 7–9 present a count of the Eigen modes below a given frequency for each of the considered building models. Firstly, mode counts for House 2-2-1 with module size $(L \times H \times W) = (4.80 \times 3.00 \times 4.80)$ m^3 and different distances between studs and joists are provided in Figure 7. As expected, the number of modes present in the building below a certain frequency is generally increasing with an increase of the rib distance. The trend is most pronounced at frequencies above 240 Hz, where the plates may baffle between two adjacent studs in the case with joist and stud distances of 600 mm. However, it may be observed that exceptions to the general trend occur, for example, at frequencies near 220 Hz. Here, more modes are present in the model with a rib distance of 400 mm compared to the model with the higher rib distance of 600 mm. This may be explained by the fact that the additional mass provided by the increased number of ribs reduces the Eigen frequencies related to some modes more than the increase

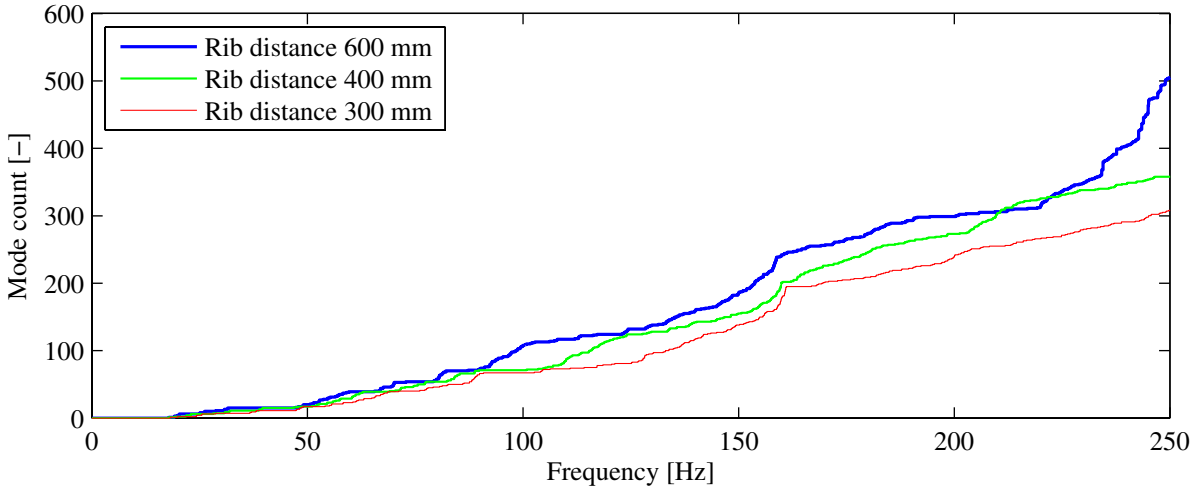

Figure 7: Eigen mode count in House 2-2-1 with module lengths $(L \times H \times W) = (4.80 \times 3.00 \times 4.80)$ m^3 and various rib distances.

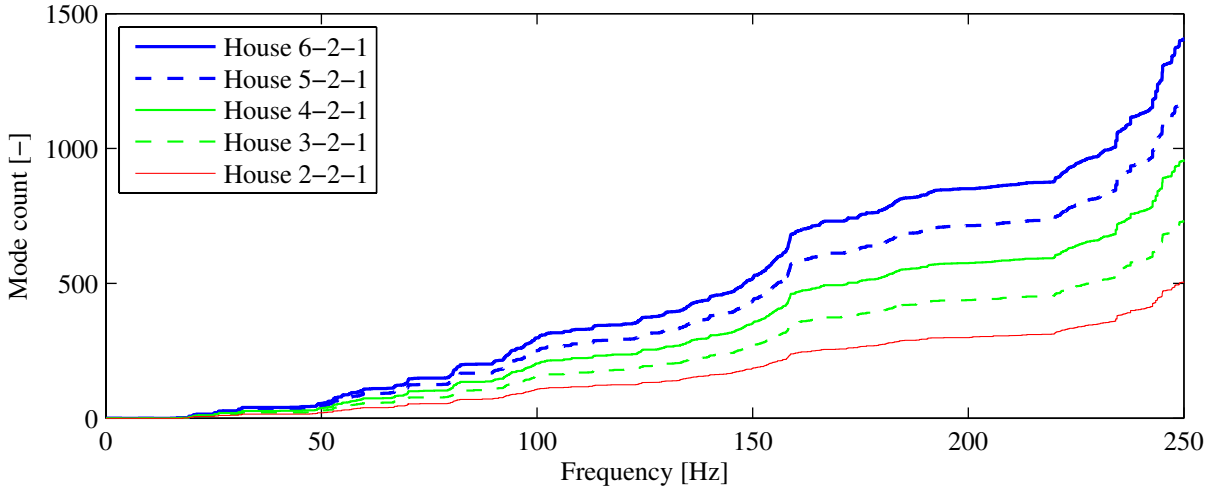

Figure 8: Eigen mode count in buildings with different numbers of modules in the x-direction. The module size is $(L \times H \times W) = (4.80 \times 3.00 \times 4.80)$ m^3, and the rib distance is 600 mm.

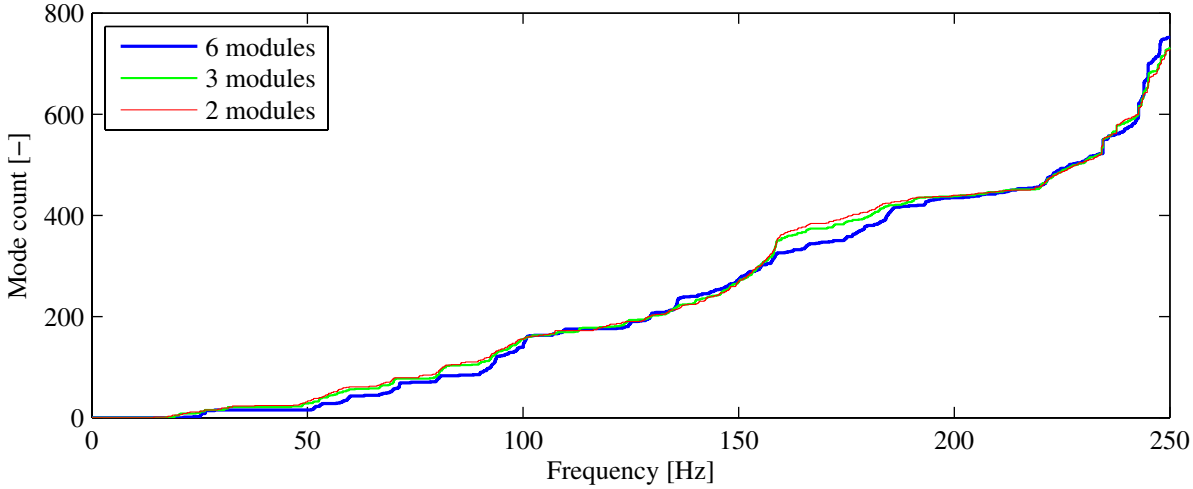

Figure 9: Eigen mode count of House N-2-1, where $N = 6, 3, 2$ is the number of modules in the x-direction. The length of the building is 14.40 m, the module size is $(L \times H \times W) = (14.40/N \times 3.00 \times 4.80)$ m^3, and the rib distance is 600 mm.

provided by the additional stiffness. The opposite effect is clearly seen at frequencies near 100 Hz and, to lesser extent, at frequencies close to 160 Hz.

Figure 8 shows the mode count in five buildings with different numbers of modules in the x-direction. The module size is in all cases $(L \times H \times W) = (4.80 \times 3.00 \times 4.80)$ m^3, and the joist and stud distances are 600 mm. It is noted that the curve for House 2-2-1 in Figure 8 is identical to the curve for a rib distance of 600 mm in Figure 7. Further, it can be observed that the number of modes is almost directly proportional to the number of modules along the building. For example, House 4-2-1 has approximately twice as many modes at all frequencies compared to House 2-2-1. This is due to the fact that only few global modes are present in the considered range of frequencies. Hence, most of the modes are related to local vibrations in the wall and floor panels.

Finally, Figure 9 provides the mode count for three different buildings: House 6-2-1, House 3-2-1 and House 2-2-1. All buildings have a length of 14.40 m, and the module size is $(L \times H \times W) = (14.40/N \times 3.00 \times 4.80)$ m^3, where $N = 6, 3, 2$ is the number of modules along the x-direction. The rib distance is 600 mm. It is observed that the number of modes is nearly the same in all three models, i.e. the number of divisions in the x-direction has marginal influence on the mode count. In the frequency ranges 50–100 Hz and, in particular, 160–190 Hz, the building with few but long modules provides the higher mode count. As opposed to this, more modes are identified in the building with six modules at frequencies near 140 Hz and again at 245 Hz. In this context it may be important to note that the z-walls each have two local modes at 138 Hz and six modes in the frequency range between 242 Hz and 247 Hz. The total number of such modes increases linearly with the number of z-wall panels in the building.

3.2 Steady-state response to harmonic excitation

Figures 10–12 show the steady state RMS velocity response of House 2-2-1 with the module size $(L \times H \times W) = (4.80 \times 3.00 \times 4.80)$ m^3 and three different rib distances. The load is applied as a vertical harmonically varying point force at the retained node placed in the middle of Floor 1-2-1, i.e. the floor of Room 1-2-1 with reference to Figure 1. At frequencies below 20 Hz, no modes exist in any of the buildings. Hence, the response corresponds to quasi-static loading of Floor 1-2-1, and there is a pronounced loss (about 50 dB) from Room 1-2-1 to Room 2-2-1. In Room 1-2-1, the velocities peak at the first few resonance modes of the floor. These modes are also excited in the next room, but with a loss of 10–20 dB.

In the frequency range 70–90 Hz, a relatively high response is observed for the floor to which the load is applied. This peak is a combination of several modes of resonance that are excited by the point force. However, the vibrations in these modes are not all transmitted with equal strength to the neighbouring room. As a result, the peak shifts to a slightly lower frequency in Room 2-2-1. From 120 Hz to 170 Hz, a significant response of Floor 1-2-1 is identified. The pass band is related to global modes that are present in all models. On the other hand, a number of pass bands and stop bands are visible in the frequency range 20-120 Hz, where the loss from Room 1-2-1 to Room 2-2-1 depends significantly on the rib distance. Differences of more than 30 dB occur, and all three models provide the higher loss at some frequencies. Thus, none of the considered rib distances is unconditionally better than the other distances.

Next, Figure 13–18 present the steady state results for five buildings, House N-2-1, with $N = 6, 5, 4, 3$ or 2 modules in the x-direction. The module size $(L \times H \times W) = (4.80 \times 3.00 \times 4.80)$ m^3 and the rib distance 600 mm have been used in all the models, and the harmonically varying vertical point force is applied in the middle of Floor 1-2-1. Firstly, in Figure 13 it is observed that the response of the loaded floor is nearly independent of the number of module repetitions

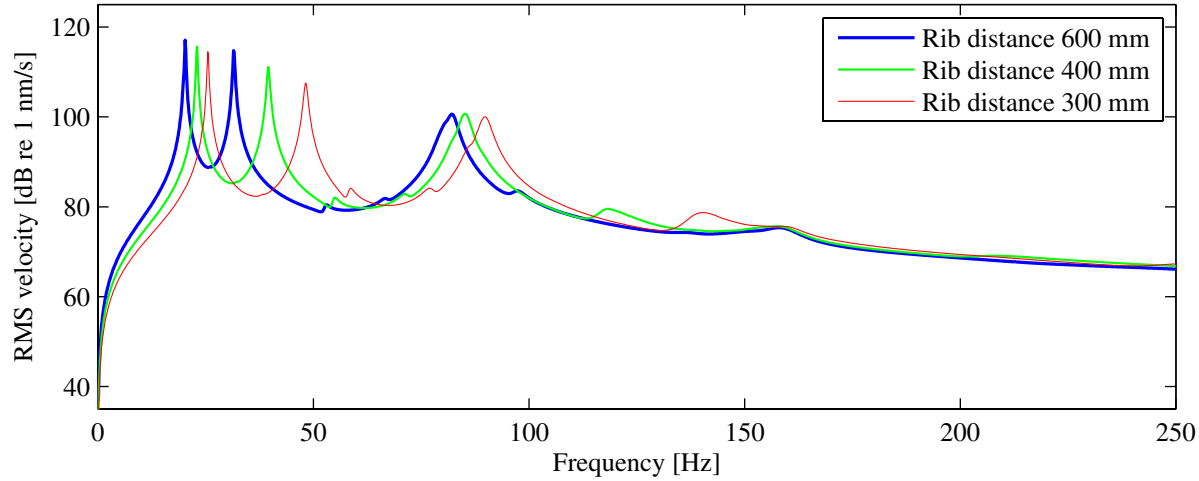

Figure 10: Steady state response in House 2-2-1 (module size $(L \times H \times W) = (4.80 \times 3.00 \times 4.80)$ m^3); RMS velocities of Floor 1-2-1 due to harmonic vertical point force excitation in the middle of Floor 1-2-1.

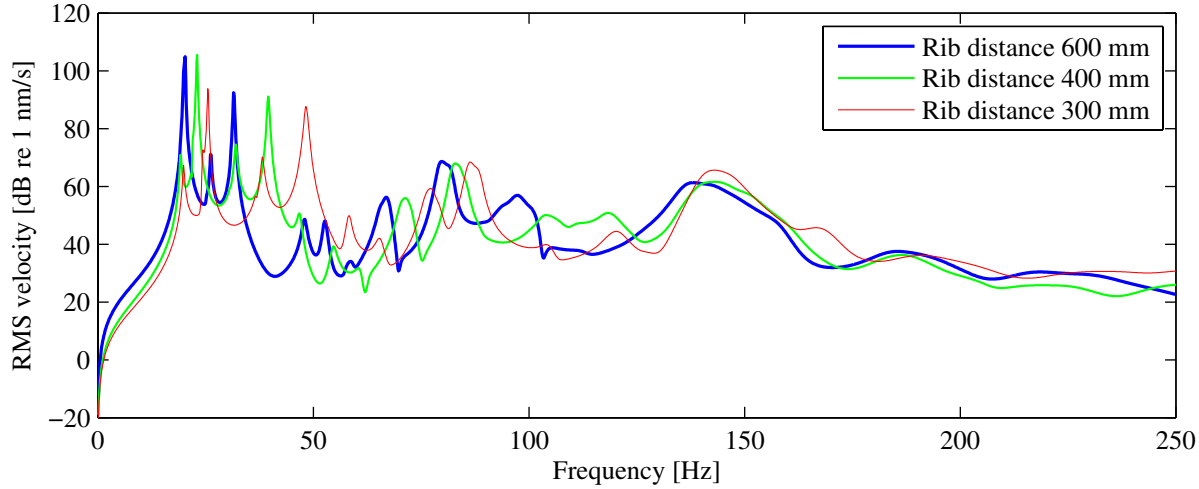

Figure 11: Steady state response in House 2-2-1 (module size $(L \times H \times W) = (4.80 \times 3.00 \times 4.80)$ m^3); RMS velocities of Floor 2-2-1 due to harmonic vertical point force excitation in the middle of Floor 1-2-1.

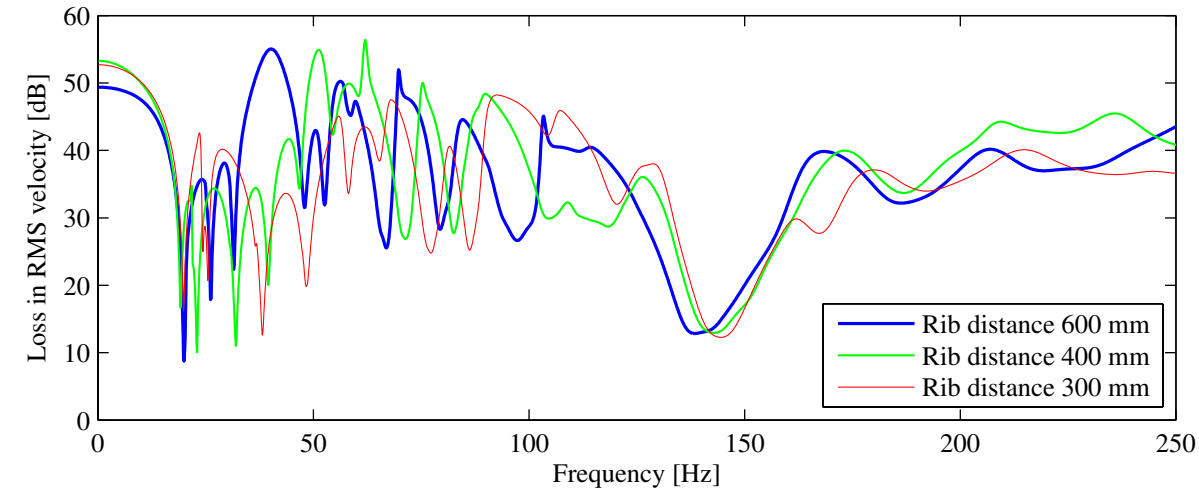

Figure 12: Steady state response in House 2-2-1 (module size $(L \times H \times W) = (4.80 \times 3.00 \times 4.80)$ m^3); loss in RMS velocities from Floor 1-2-1 to Floor 2-2-1 due to harmonic vertical point force excitation in the middle of Floor 1-2-1.

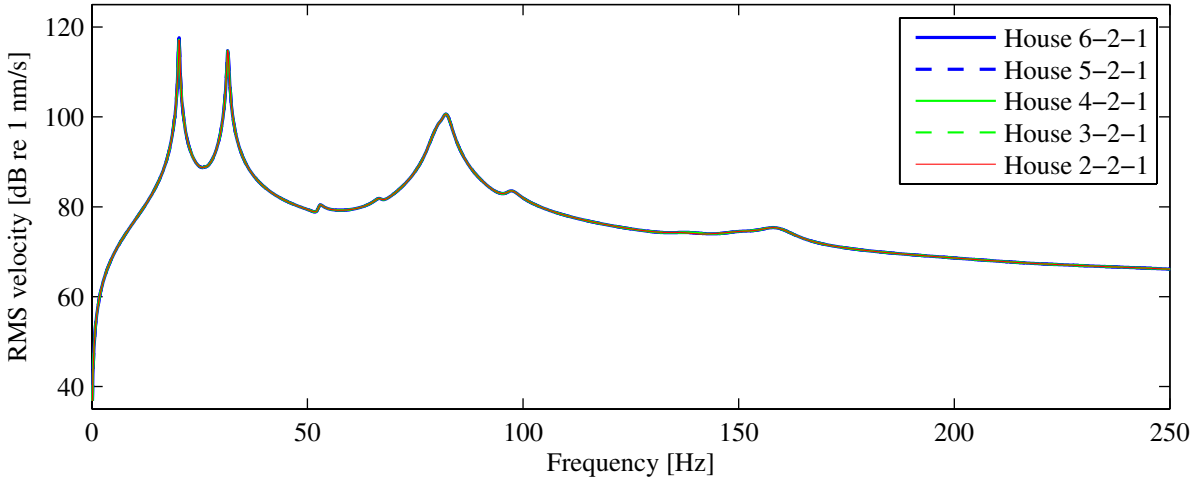

Figure 13: Steady state response in different buildings (module size $(L \times H \times W) = (4.80 \times 3.00 \times 4.80)$ m^3, rib distance 600 mm); RMS velocities of Floor 1-2-1 due to harmonic vertical excitation in the middle of Floor 1-2-1.

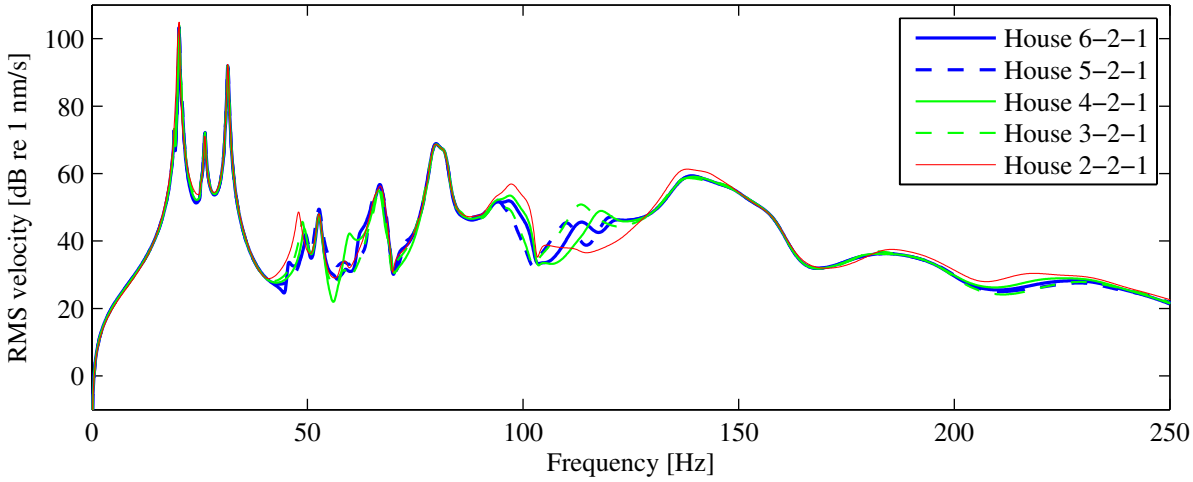

Figure 14: Steady state response in different buildings (module size $(L \times H \times W) = (4.80 \times 3.00 \times 4.80)$ m^3, rib distance 600 mm); RMS velocities of Floor 2-2-1 due to harmonic vertical excitation in the middle of Floor 1-2-1.

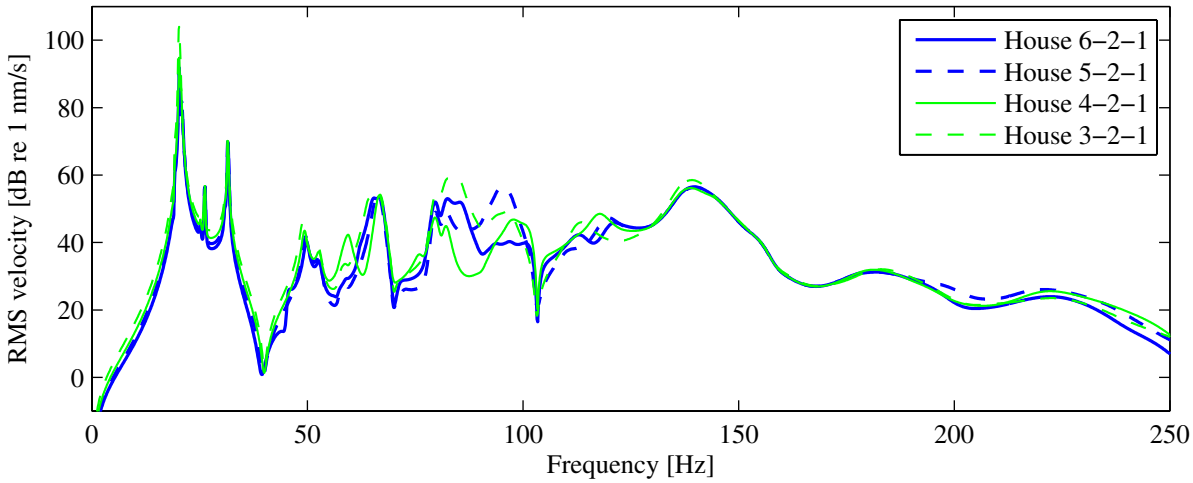

Figure 15: Steady state response in different buildings (module size $(L \times H \times W) = (4.80 \times 3.00 \times 4.80)$ m^3, rib distance 600 mm); RMS velocities of Floor 3-2-1 due to harmonic vertical excitation in the middle of Floor 1-2-1.

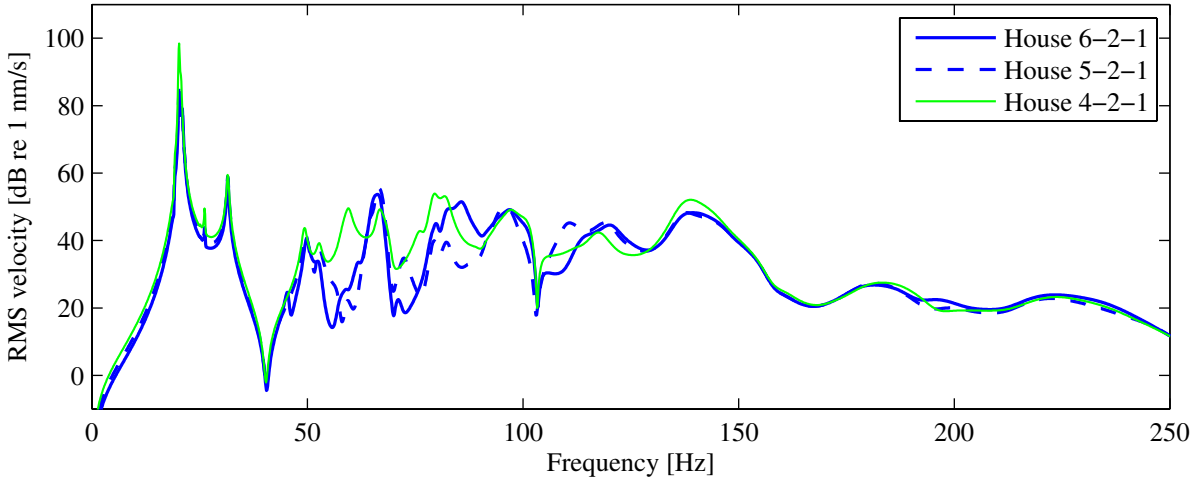

Figure 16: Steady state response in different buildings (module size $(L \times H \times W) = (4.80 \times 3.00 \times 4.80)$ m^3, rib distance 600 mm); RMS velocities of Floor 4-2-1 due to harmonic vertical excitation in the middle of Floor 1-2-1.

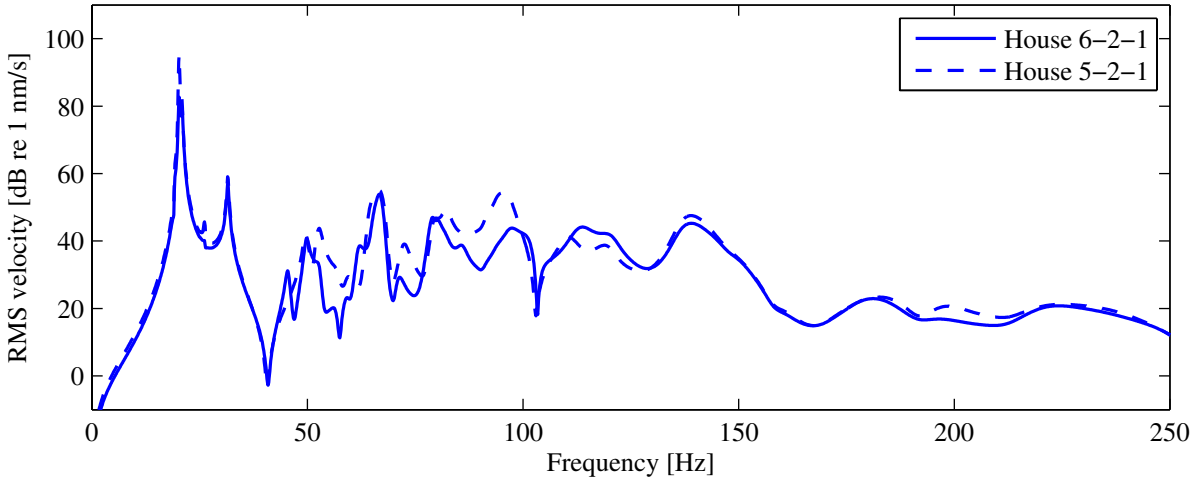

Figure 17: Steady state response in different buildings (module size $(L \times H \times W) = (4.80 \times 3.00 \times 4.80)$ m^3, rib distance 600 mm); RMS velocities of Floor 5-2-1 due to harmonic vertical excitation in the middle of Floor 1-2-1.

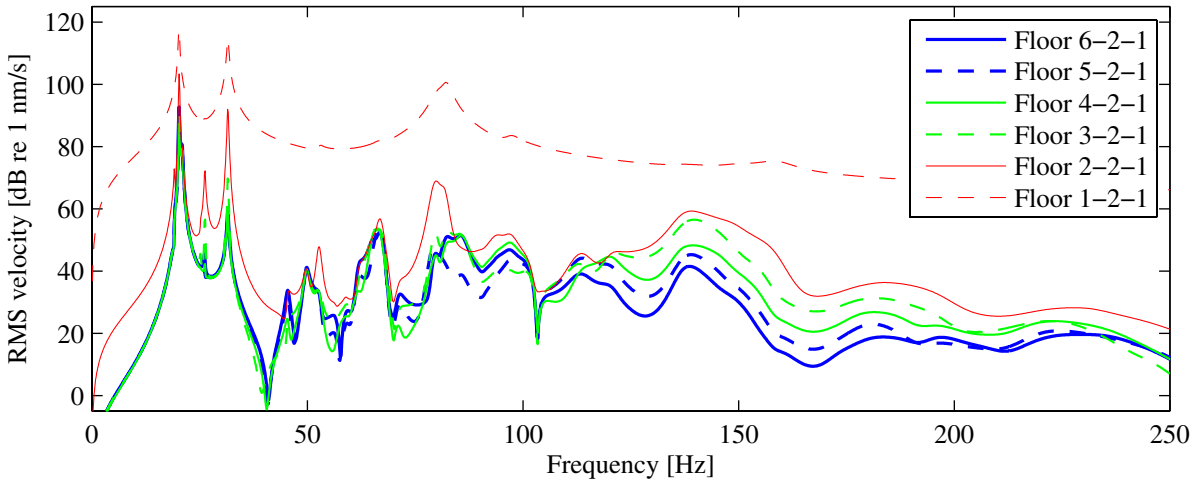

Figure 18: Steady state response in House 6-2-1 (module size $(L \times H \times W) = (4.80 \times 3.00 \times 4.80)$ m^3, rib distance 600 mm); RMS velocities of different floors due to harmonic vertical excitation in the middle of Floor 1-2-1.

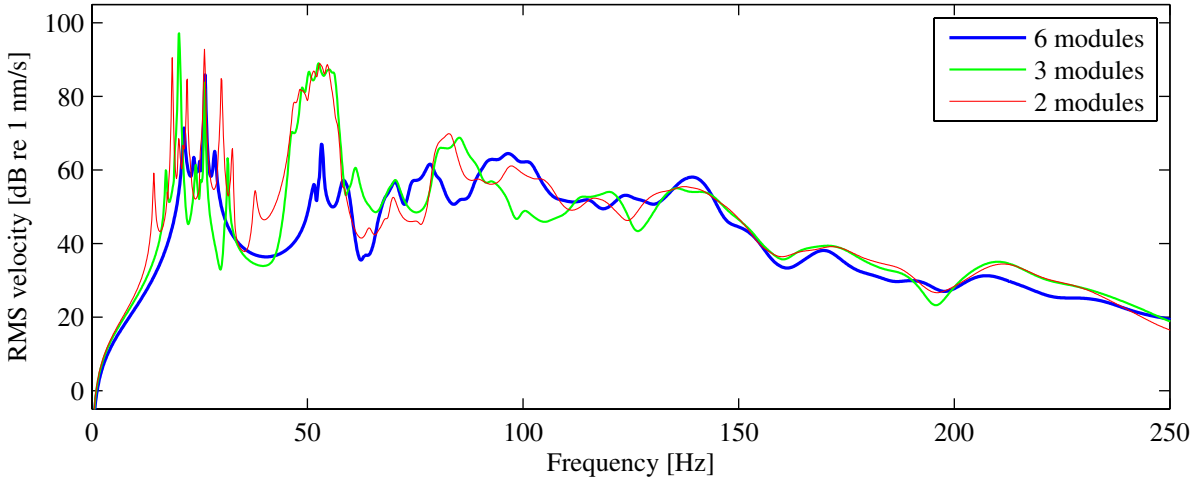

Figure 19: Steady state response in House N-2-1, where $N = 6, 3, 2$ is the number of modules in the x-direction. The length of the building is 14.40 m, the module size is $(L \times H \times W) = (14.40/N \times 3.00 \times 4.80)$ m^3, and the rib distance is 600 mm; RMS velocities of three points in the right end of the building due to harmonic vertical excitation at the point $(x, z) = (1.20, 1.20)$ m^2 on Floor 1-2-1.

along the building. From the subsequent figures it may be concluded that the response in other rooms is also only weakly influenced by the number of modules present in the x-direction. The most significant differences in RMS velocity response occur in the frequency range 40–120 Hz. Here, the response is up to 20 dB higher in some models compared to the response in other models. No clear conclusion can be made whether a building with more modules will provide smaller or larger responses. For example, in some floors and within certain frequency intervals, House 4-2-1 provides a higher RMS velocity level than House 6-2-1, whereas the opposite trend can be seen for other floors or frequencies. On the other hand, in Figure 18 it can be observed that the response in House 6-2-1 is generally decreasing with the distance away from the loaded floor, i.e. the RMS velocities of Floor 6-2-1 are lower than the RMS velocities of Floor 5-2-1, which are again lower than the RMS velocities of Floor 4-2-1 and so on. The trend is particularly clear in the frequency range 120–180 Hz.

Finally, the steady state response in three different buildings of the same length, 14.40 m, are visualized in Figure 19. The response is computed as the RMS value of the velocities in the three retained floor nodes which are as far away from the load as possible. The harmonically varying vertical point force is applied to Floor 1-2-1 at the retained node with coordinates $(x, z) = (1.20, 1.20)$ m^2. The module size is $(L \times H \times W) = (14.40/N \times 3.00 \times 4.80)$ m^3, where $N = 6, 3, 2$ is the number of modules in x-direction, and the rib distance is 600 mm. It should be noted that nonstructural mass has been added only to the retained degrees of freedom on the top surfaces of the floor panels. There are 15 such points on the floor panels with dimensions $(L \times W) = (7.20 \times 4.80)$ m^2 and only three points on the floors with dimensions $(L \times W) = (2.40 \times 4.80)$ m^2. However, the mass of a z-wall panel is about 220 kg which is only slightly less than the 300 kg of nonstructural mass it replaces. As a consequence, the total masses of the three buildings are nearly the same; but the stiffnesses are different.

It may be observed in Figure 19 that a stop band exists in the frequency range around 40 Hz. The width of this stop band increases significantly with the number of divisions in the x-direction. However, at frequencies near 100 Hz the model with six modules provide the higher response. Hence, the results a ambiguous regarding the effect of adding more periodic divisions into the same building.

3.3 Transient response to a step load on a floor

The transient responses obtained by time-domain analyses of the various considered buildings are presented in Figures 20–28. Results of the analyses with different rib distances are provided in Figures 20 and 21, whereas Figures 22–27 show the results of the analyses with different numbers of modules of the same size. Finally, Figure 25 visualizes the response in the three buildings with the same overall length but different numbers of divisions in the x-direction.

In Figure 20 it can be seen that the maximum response of the loaded Floor 1-2-1 occurs immediately after the application of the step load which has a duration of 20 ms. The response of the floor in the model with a rib distance of 300 mm is slightly smaller than the response of the floor in the model with a rib distance of 400 mm and even smaller than the response in the model with a rib distance of 600 mm. The results for the rib distance of 300 mm contain an apparent low-frequency vibration with a frequency of about 3 Hz. However, no mode with such a low frequency has been identified for the building model. Hence, the phenomenon must be caused by modulation due to two (or more) closely spaced modes vibration at higher

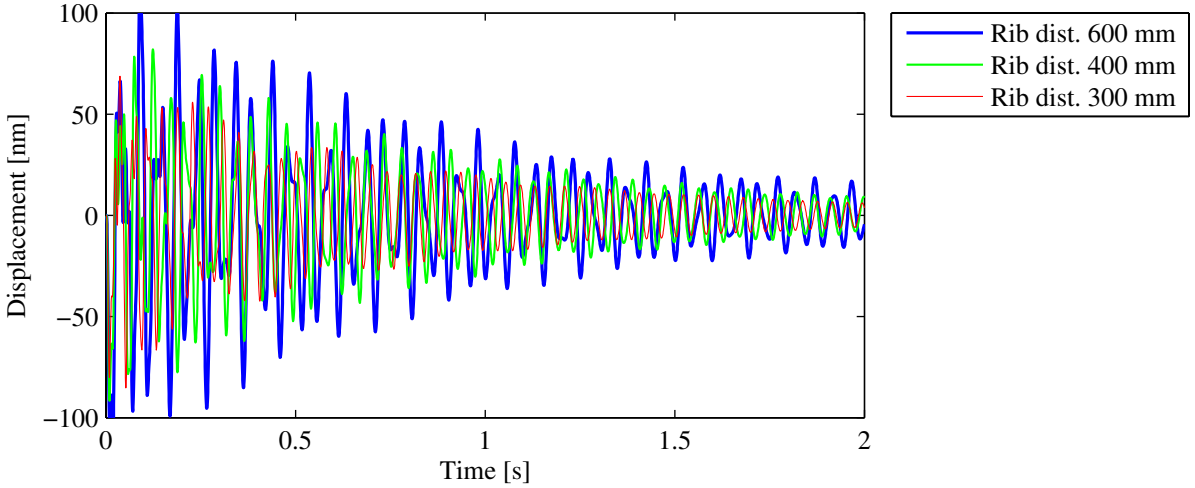

Figure 20: Transient response in House 2-2-1 (module size $(L \times H \times W) = (4.80 \times 3.00 \times 4.80)$ m^3); vertical displacement in the middle of Floor 1-2-1 due to a vertical step load in the middle of Floor 1-2-1.

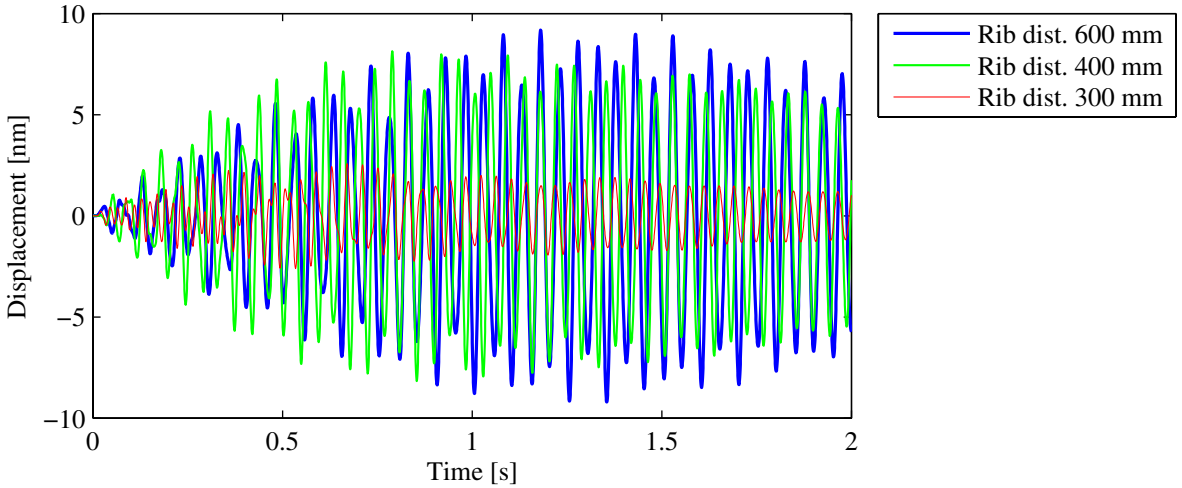

Figure 21: Transient response in House 2-2-1 (module size $(L \times H \times W) = (4.80 \times 3.00 \times 4.80)$ m^3); vertical displacement in the middle of Floor 2-2-1 due to a vertical step load in the middle of Floor 1-2-1.

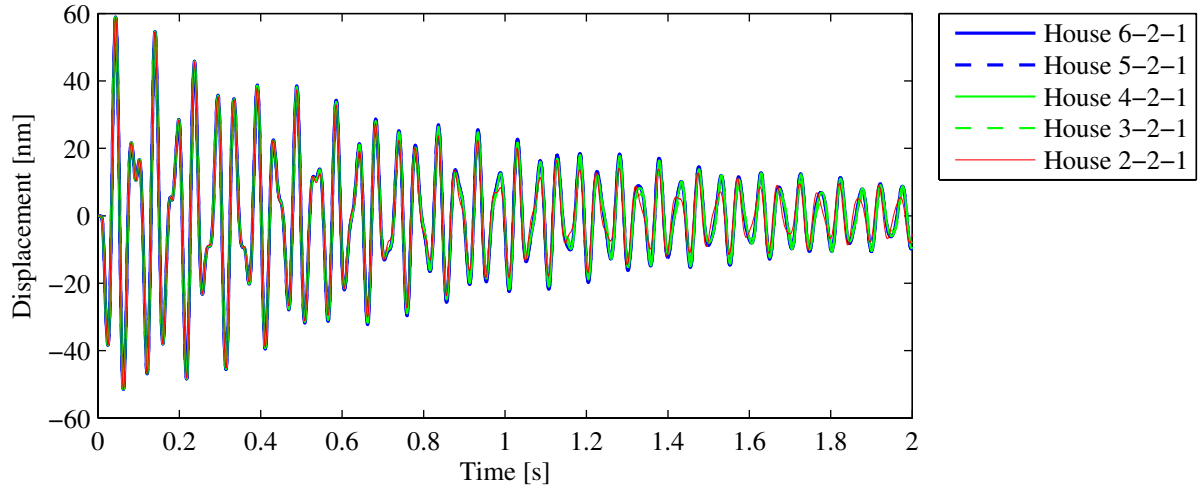

Figure 22: Transient response in different buildings with module size $(L \times H \times W) = (4.80 \times 3.00 \times 4.80)$ m^3 and rib distance 600 mm; vertical displacement in the middle of Floor 1-2-1 due to a vertical step load in the middle of Floor 1-2-1.

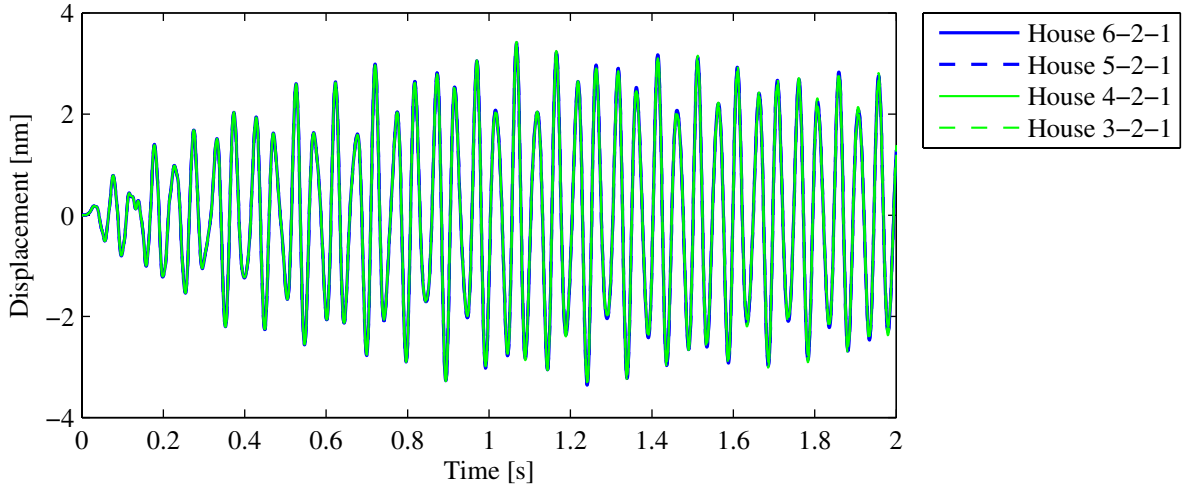

Figure 23: Transient response in different buildings with module size $(L \times H \times W) = (4.80 \times 3.00 \times 4.80)$ m^3 and rib distance 600 mm; vertical displacement in the middle of Floor 2-2-1 due to a vertical step load in the middle of Floor 1-2-1.

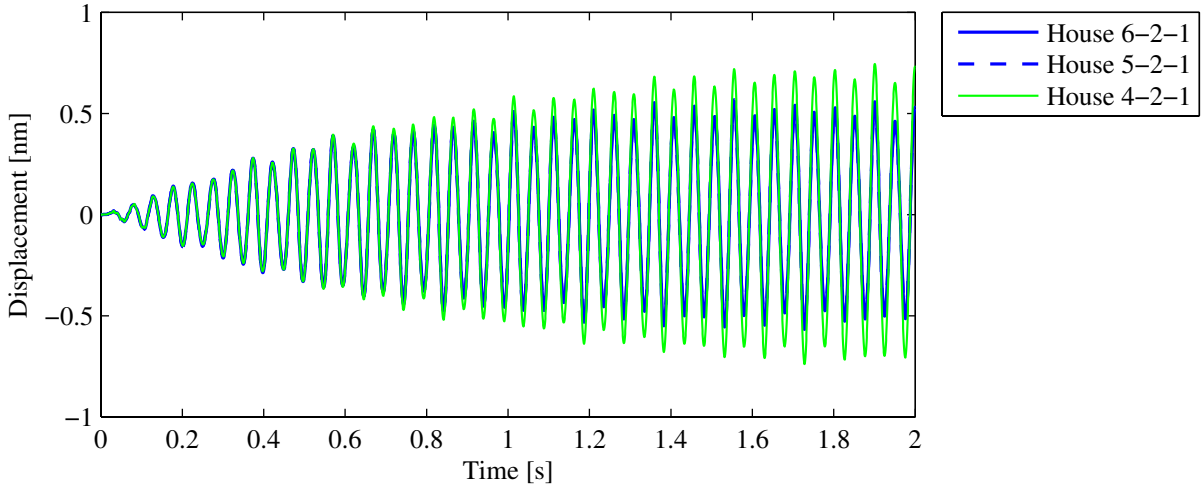

Figure 24: Transient response in different buildings with module size $(L \times H \times W) = (4.80 \times 3.00 \times 4.80)$ m^3 and rib distance 600 mm; vertical displacement in the middle of Floor 3-2-1 due to a vertical step load in the middle of Floor 1-2-1.

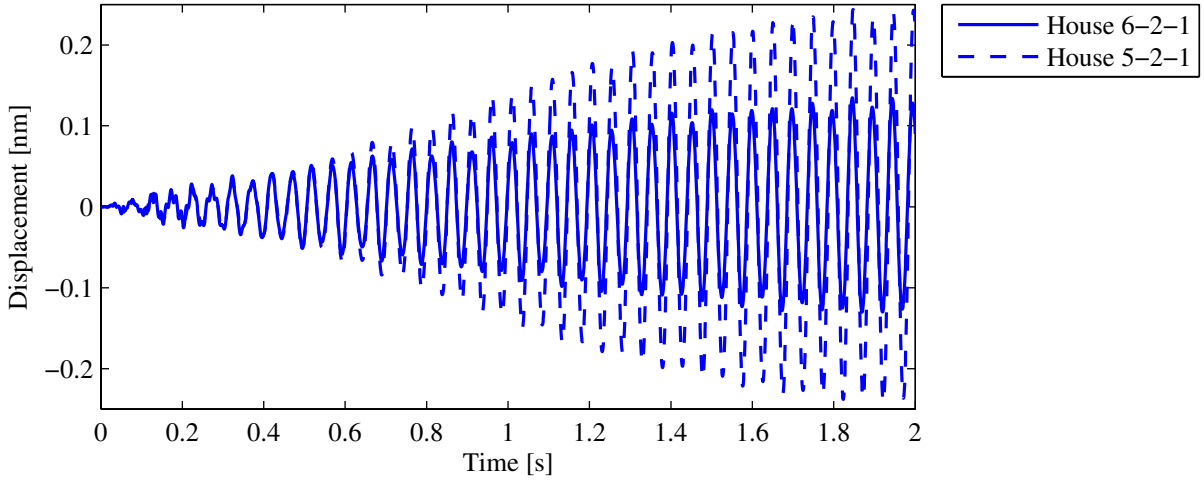

Figure 25: Transient response in different buildings with module size $(L \times H \times W) = (4.80 \times 3.00 \times 4.80)$ m^3 and rib distance 600 mm; vertical displacement in the middle of Floor 4-2-1 due to a vertical step load in the middle of Floor 1-2-1.

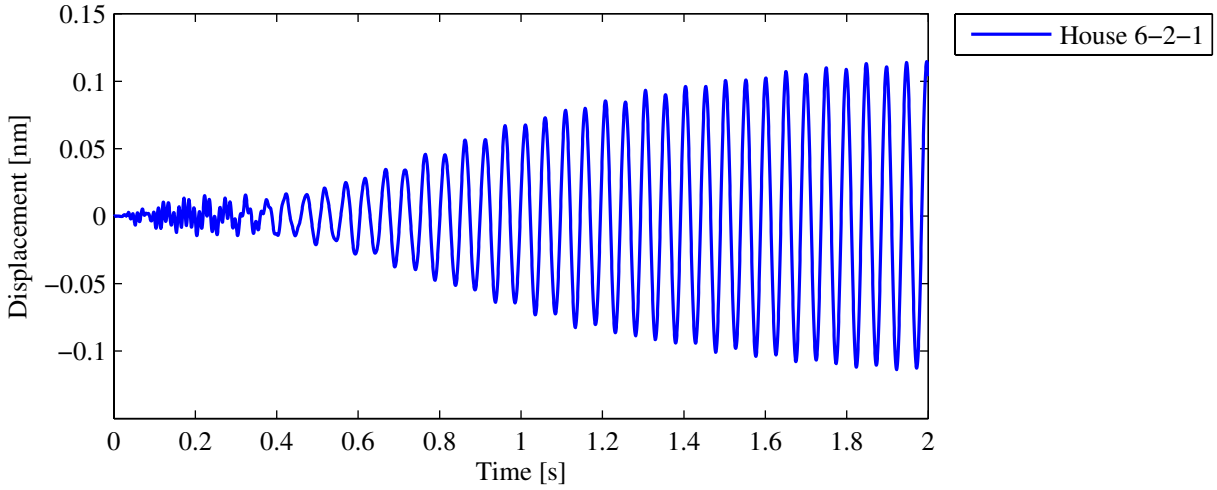

Figure 26: Transient response in House 6-2-1 and module size $(L \times H \times W) = (4.80 \times 3.00 \times 4.80)$ m^3 with rib distance 600 mm; vertical displacement in the middle of Floor 5-2-1 due to a vertical step load in the middle of Floor 1-2-1.

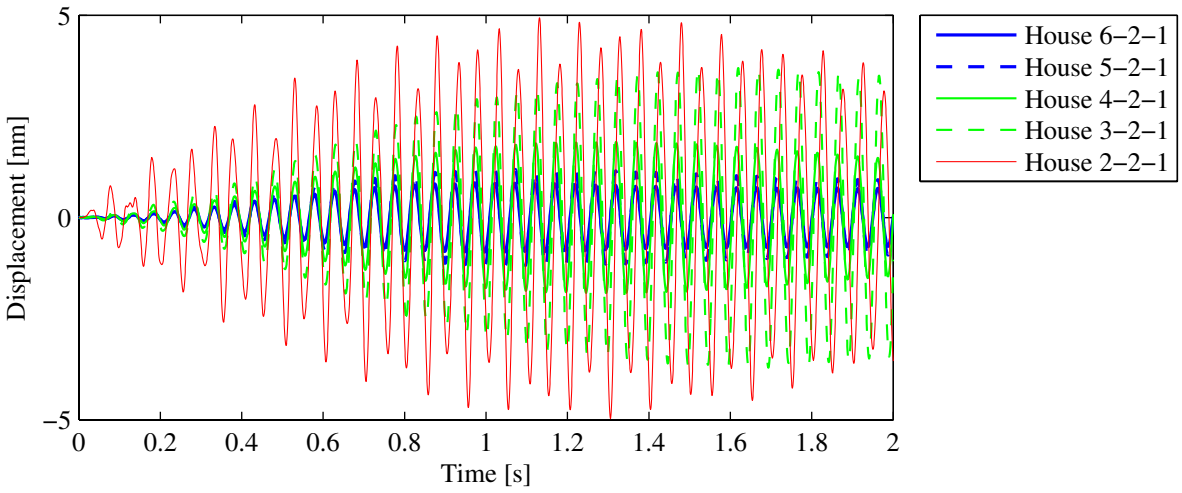

Figure 27: Transient response in House N-2-1, $N = 2, 3, 4, 5, 6$, with module size $(L \times H \times W) = (4.80 \times 3.00 \times 4.80)$ m^3 and rib distance 600 mm; vertical displacement in the middle of Floor N-2-1 due to a vertical step load in the middle of Floor 1-2-1.

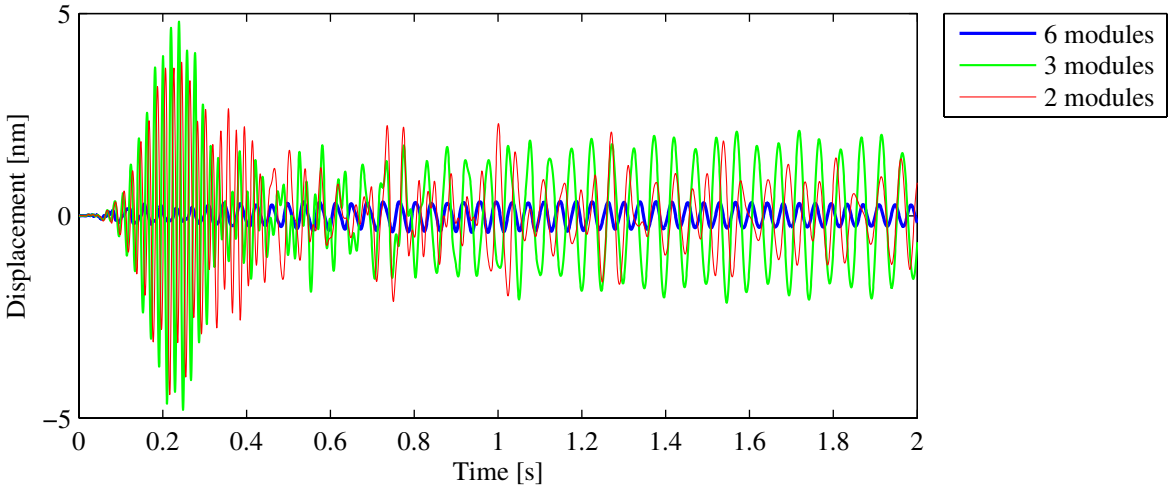

Figure 28: Transient response in House N-2-1, where $N = 6, 3, 2$ is the number of modules in the x-direction. The length of the building is 14.40 m, the module size is $(L \times H \times W) = (14.40/N \times 3.00 \times 4.80)$ m^3, and the rib distance is 600 mm; vertical displacement at the point $(x, z) = (13.20, 3.60)$ m^2 on Floor N-2-1 due to harmonic vertical excitation at the point $(x, z) = (1.20, 1.20)$ m^2 on Floor 1-2-1.

frequencies. Figure 21 reveals that the response of Floor 2-2-1 increases with time. Towards the end of the 2.0 s time interval the response is of the same magnitude in the two floors. Thus, energy is continuously transferred from Floor 1-2-1 to Floor 2-2-1. The tendency is less pronounced for the building with a rib distance of 300 mm, where the response of Floor 2-2-1 is much smaller than the responses recorded in the buildings with rib distances of 400 or 600 mm.

According to Figure 22, the response of Floor 1-2-1 is close to being identical in the five buildings with different number of modules with the same size $(L \times H \times W) = (4.80 \times 3.00 \times 4.80)$ m^3 and rib distance 600 mm. Only in the case of House 2-2-1 is there a small deviation from the other results—especially towards the end of the two-second time interval. From Figures 23–27 it can be seen that the energy introduced by the step load is gradually transferred to the other rooms. An interesting observation regards Figure 25 and especially Figure 26, where a high-frequent vibration signal is observed to appear in the first part of the response. After approximately 0.4 s, these vibrations are damped out and vibrations with a lower frequency take over. A plausible explanation is that the same number of cycles is necessary to transfer energy from one one room to another, independently of the frequency and therefore the high-frequency vibrations are visible in the far end of the building shortly after application of the load. Another essential result is observed in Figure 27 which shows the displacement response at the midpoint of the floor in the room lying in the far end of each building, as far away from the loaded floor as possible but still in the same storey. For example, the response of Floor 2-2-1 is visualized in the case of House 2-2-1, whereas the response of Floor 5-2-1 is provided for House 5-2-1. The response increases with decreasing number of modules in the x-direction. Further, by comparison with Figures 23–27 it can be seen that the response of Floor 3-2-1 of House 3-2-1 is higher than the response of the neighbouring room that lies closer to the load. Similar observations can be made regarding Floor 4-2-1 of House 4-2-1, Floor 5-2-1 of House 5-2-1, and Floor 6-2-1 of Floor 6-2-1. Thus, energy seems to accumulate in the room that lies farthest away from the load.

Finally, Figure 28 compares the vertical displacement at the point $(x, z) = (13.20, 3.60)$ m^2 on Floor N-2-1 due to harmonic vertical excitation at the point $(x, z) = (1.20, 1.20)$ m^2 on Floor 1-2-1, where $N = 6, 3, 2$ refers to the number of modules in the x-direction. In House 2-

2-1 with module size $(L \times H \times W) = (7.20 \times 3.00 \times 4.80)$ m^3 and in House 3-2-1 with module size $(L \times H \times W) = (4.80 \times 3.00 \times 4.80)$ m^3, high-frequency vibrations are transferred to the far corner of the building within the first 0.2 s. This is not the case in House 6-2-1 with module size $(L \times H \times W) = (2.40 \times 3.00 \times 4.80)$ m^3, where the vibrations in the observation point occur with a single frequency for the entire duration of the simulation. Inspection of the displacement response in the remaining floors of House 6-2-1 (not illustrated in the present paper) shows that the high-frequency vibrations are only transmitted to the first couple of rooms away from the source. Thus, a response similar to that of Floor 2-2-1 in House 2-2-1 also occurs in Floor 2-2-1 of House 6-2-1.

4 CONCLUSIONS

A number of comparisons have been made between lightweight wooden building structures with different configurations regarding rib distance, number of modules along the building and size of the module in the length direction of the building. The main findings of the present analyses are:

- A modular finite-element model with substructures generated for each wall and floor panel provides an effective platform for parametric studies of vibration transmission in a large lightweight building structure. The global models contain about 25,000 degrees of freedom, whereas a single panel model has up to 250,000 degrees of freedom before system reduction.

- The distance between studs and joists in wall and floor panels has a significant impact on the modal density in the low and mid-frequency range. Further, the rib distance strongly influences the position and width of stop bands for transmission of vibrations in the steady state. For a transient step load analysed in the time domain, some rib distances may lead to significantly smaller response than others—especially in a room adjacent to the room with excitation of the floor.

- The mode count in a lightweight wooden building structure is proportional to the number of repetitions of an identical module along the building in its length direction, since the majority of modes are related to local vibrations in floor and wall panels. The steady state response to harmonic loading is not very sensitive to the number of modules along the building. For example, the response of the loaded floor is nearly identical for buildings with two and six modules along the building. However, in a building which is several modules long, the response decreases with increasing distance away from the source, in particular in the mid-frequency range. For a step load, the vibrations are gradually transmitted from one room to another along the building. High-frequency vibrations are transmitted faster than low-frequency, but they are also damped out more rapidly.

- Buildings with the same length but divided into different numbers of modules along the building have similar numbers of Eigen modes below a given frequency. When some of the walls, dividing the building in its length direction, are removed, these wall panels will obviously not contribute to the net number of modes. However, this is compensated by an increasing number of modes in the remaining, now longer, wall and floor panels. In any case, inclusion of more walls, resulting in an increase of the number of modules and a reduction of the module size, may have a significant impact on the steady state response to harmonic loads. Hence, stop bands may change width and position. Further, the transient

response in one end of the building due to a step load in the other end of the building depends strongly on the number of modules. For example, high-frequency vibrations may not reach the far end of the building when many walls divide the building in its length direction, whereas strong vibrations occur when only one or two walls intersect the transmission path.

It should finally be mentioned that the analyses have all been based on the assumption of linear viscous material dissipation, implemented in terms of Rayleigh damping. About one to two percent of critical damping has been assumed in the considered frequency range, which may be low for a building structure with frictional joints and nonstructural elements. In future research and further development of the modular building finite-element model, more realistic damping models and damping levels should be identified and implemented.

ACKNOWLEDGEMENT

The present research is part of the Interreg project "Silent Spaces", funded by the European Union. The authors highly appreciate the financial support.

REFERENCES

[1] R. Craik, *Sound Transmission Through Buildings: Using Statistical Energy Analysis*. Gower, Aldershot, 1996.

[2] European Committee for Standardization, *EN 12354-1:2000 Building Acoustics. Estimation of Acoustic Performance in Buildings from the Performance of Elements. Airborne Sound Insulation between Rooms (3rd ed.)*. European Committee for Standardization, 2000.

[3] J. Mahn, *Prediction of flanking noise transmission in lightweight building constructions: A theoretical and experimental evaluation of the application of EN12354-1*. Technical report, University of Canterbury, Acoustics Research Group, 2007.

[4] D.J. Mead, Wave propagation in continuous periodic structures: Research contributions from Southampton, 1964-1995. *Journal of Sound and Vibration*, **190**(3), 495-524, 1996.

[5] J. Brunskog P. Davidsson (2004), Sound transmission of structures. A finite element approach with simplified room description. *Acta Acustica united with Acustica*, **90**, 847–857, 2004.

[6] F. Løvholt, C. Madshus, K. Norén-Cosgriff, Analysis of low frequency sound and sound induced vibration in a Norwegian wooden building. *Noise Control Engineering Journal*, **59**(4), 383–396, 2011.

[7] S. Maluski, B. Gibbs, Application of a finite-element model to low-frequency sound insulation in dwellings. *Journal of the Acoustical Society of America*, **108**(4), 1741–1751, 2000.

[8] P. Fiala, G. Degrande, F. Augusztinovicz, Numerical modelling of ground-borne noise and vibration in buildings due to surface rail traffic. *Journal of Sound and Vibration*, **301**, 718–738, 2007.

[9] L.V. Andersen, P.H. Kirkegaard, K. Persson, B. Niu, A modular finite element model for analysis of vibration transmission in multi-storey lightweight buildings (Paper 189). B. Topping (Ed.), Proceedings of the Eleventh International Conference on Computational Structures Technology, *Civil-Comp Proceedings*, **99**, Civil-Comp Press, Stirlingshire, Scotland, 2012.

[10] Dassault Systèmes Simulia Corp., *Abaqus 6.12 Analysis User's Manual*, Dassault Systèmes Simulia Corp., Providence, RI, USA, 2012.

[11] R. Craig M. Bambton, Coupling of substructures for dynamic analysis. *AIAA Journal*, **6**(7), 1313–1319, 1968.

[12] R. Craig, *Structural dynamics: An introduction to computer methods*. John Wiley & Sons Inc., New York, 1981.

[13] R. Guyan, Reduction of stiffness and mass matrices. *AIAA Journal*, **3**(2), 380, 1965.

[14] N. Kiel, L.V. Andersen, N. Niu, K. Persson, Different modelling approaches to coupling wall and floor panels within a dynamic finite element model of a lightweight building (Paper 190). B. Topping (Ed.), Proceedings of the Eleventh International Conference on Computational Structures Technology, *Civil-Comp Proceedings*, **99**, Civil-Comp Press, Stirlingshire, Scotland, 2012.

[15] N.M. Newmark, A method of computation for structural dynamics. *ASCE Journal of the Engineering Mechanics Division*, **85**(EM3), 67–94, 1959.